Synthesis and spectroscopic and thermogravimetric characterization of heterobimetallic complexes with Sn(IV) and Pd(II); DNA binding, alkaline phosphatase inhibition and biological activity studies

Shabbir Hussain, Iftikhar Hussain Bukhari, Saqib Ali, Saira Shahzadi, Muhammad Shahid & Khurram Shahzad Munawar

Taylor & Francis
Taylor & Francis Group

Synthesis and spectroscopic and thermogravimetric characterization of heterobimetallic complexes with Sn(IV) and Pd(II); DNA binding, alkaline phosphatase inhibition and biological activity studies

SHABBIR HUSSAIN*†, IFTIKHAR HUSSAIN BUKHARI†, SAQIB ALI‡,
SAIRA SHAHZADI†, MUHAMMAD SHAHID§ and
KHURRAM SHAHZAD MUNAWAR‡

†Department of Chemistry, GC University, Faisalabad, Pakistan
‡Department of Chemistry, Quaid-i-Azam University, Islamabad, Pakistan
§Department of Chemistry and Biochemistry, University of Agriculture, Faisalabad, Pakistan

A palladium complex and its heterobimetallic (Sn, Pd) derivatives were synthesized and characterized by spectroscopic and thermogravimetric analyses. The palladium complex showed higher potential to bind with SS-DNA and to inhibit the alkaline phosphatase (ALPs) relative 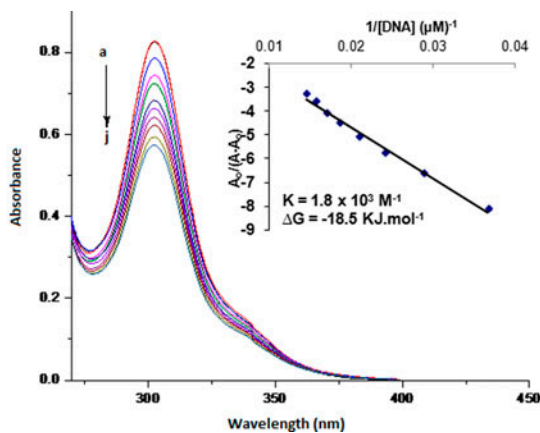to the heteronuclear products (**2–7**). However, the bimetallic derivatives displayed significantly higher antifungal/antibacterial activities than the palladium complex **1**.

A palladium complex, $[KLCSS]_2Pd$ (**1**), has been prepared by stirring sarcosine (HLH), KOH and CS_2 in methanol and subsequently treating with palladium(II) chloride. Six heterobimetallic derivatives of the type $[R_2(Cl)SnLCS_2]_2Pd$ (R = Me: **2**; Bu: **3**; Ph: **4**)/$[R_3SnLCS_2]_2Pd$ (R = Me: **5**; Bu: **6**; Ph: **7**) were also synthesized by stirring sarcosine (HLH) with KOH and CS_2 in methanol followed by an addition of R_2SnCl_2/R_3SnCl and then $PdCl_2$. FT-IR data demonstrated bidentate binding of

---

*Corresponding author. Email: shabchem786@gmail.com

dithiocarbamate and carboxylate with four- and five-coordinate environments around Pd(II) and Sn(IV) centers, respectively, in the solid state. UV–visible studies verified the square planar arrangement around Pd(II) in solution. The magnitude of $^2J(^{119}Sn-^1H)$ demonstrates a distorted trigonal bipyramidal geometry around tin(IV) in solution. Elemental analysis (C, H, N, and S), mass spectroscopic (EI-MS and ESI), and thermogravimetric analyses verified the chemical composition of products. Complexes **1–7** exhibited interaction with salmon sperm DNA (SS-DNA). The palladium complex **1** had shown higher potential to bind with SS-DNA and to inhibit the alkaline phosphatase when compared to the heteronuclear products (**2–7**). However, the antifungal/antibacterial activities of the bimetallic complexes (**2–7**) were significantly higher than the palladated derivative **1**. The *in vitro* hemolytic activity investigations on human red blood cells showed that bimetallic derivative **2** with chlorodimethyltin(IV) exhibited the lowest hemolytic effects (17.55%), while **5** having trimethyltin(IV) center exhibited the highest hemolytic activity (78.64%).

Keywords: Heterobimetallic; Sarcosine; Spectroscopic; TGA; Geometry; SS-DNA; Alkaline phosphatase; Antifungal/antibacterial; Hemolytic

1. Introduction

Heterobimetallic complexes have applications in photochemical molecular devices and as light sensitive probes in biological systems [1]. Asymmetric Diels–Alder reactions proceed efficiently in the presence of the heterobimetallic catalysts [2]. As such complexes behave as both a Brønsted base and as a Lewis acid, just like an enzyme, they make possible a variety of efficient catalytic asymmetric reactions. The two different metals may play different roles to enhance the reactivity of both reaction partners and to position them [3]. The presence of two metal ions in close proximity mimics the active site of several metalloproteins and metalloenzymes and offers an opportunity to study metal–proteins and metal–enzyme interactions [4].

Heteronuclear chemistry that joins palladium and tin moieties may be fascinating. Many organotin and organopalladium complexes with various ligands have been synthesized and characterized due to their broad range of applications in various fields, i.e. pharmaceutical, industrial, and agricultural [5–15]. Organotin(IV) complexes have been used in industry as catalysts for esterification and transesterification [5], PVC stabilization [6], and as ion carriers in electrochemical membrane design [7]. They have also been known for biological properties against bacterial, fungal strains, and cancer cells line [8, 9]. Dichloro(protoporphyrin) tin(IV) may be used to prevent neonatal jaundice which causes neurotoxic symptoms [10]. Pd(II) complexes of various ligands possess antiviral, malarial, fungal, and microbial activities [11]. There are reports on luminescence, antibacterial, and catalytic activities of palladium(II) complexes with Schiff bases [12]. Recently, DNA-binding properties of Pd(II) and Pt(II) dithiocarbamates have attracted attention of many researchers, and their potential antitumor properties have been investigated [13, 14]. The complexes are less toxic, more stable, and had more specific antitumor activity *in vivo* [15].

With the significance of organotin and organopalladium complexes, it may be very important to introduce both Pd and Sn into a polyfunctional ligand and examine its properties as a heterobimetallic product. The purpose of this study is to coordinate oxygen and sulfur sites of potassium 2-(dithiocarboxylato(methyl)amino)acetate with tin(IV) and palladium(II) centers and investigate the biological potential of the consequent multinuclear complexes. The use of elemental analysis, spectroscopic techniques (IR, UV–visible, ^1H and ^{13}C NMR, EI-MS and ESI), and thermogravimetric analyses (TGA) enables the detailed studies of structures including chemoselectivity, coordination modes, and geometries around Pd(II) and

Sn(IV) centers in the solid and solution states of the complexes. The efficacy of the products has been tested by investigating their interaction with salmon sperm DNA and potential ability to inhibit the alkaline phosphatase (ALPs) enzyme. The antimicrobial actions of the complexes were assessed by screening them against various strains of bacteria/fungi, and the minimal inhibitory concentrations were also evaluated. The effect of Pd and Sn on the biopotencies of complexes has been compared and the structure activity relationships have also been explored. *In vitro* hemolytic activities were performed to see possible toxic effects on human red blood cells.

2. Experimental

2.1. *Materials and methods*

Dimethyltin dichloride, dibutyltin dichloride, diphenyltin dichloride, trimethyltin chloride, tributyltin chloride, triphenyltin chloride, palladium chloride, carbon disulphide, *p*-nitrophenyl phosphate hexahydrate, diethanolamine, and magnesium chloride were purchased from Sigma–Aldrich (USA) and used without purification. Sarcosine (HLH) was procured from Merck (Germany). From Oxoid, Hampshire, UK, nutrient agar, nutrient broth, potato dextrose agar, and sabouraud dextrose agar were bought. Human serum was used as a source of ALPss. AR-grade solvents of Merck (methanol), Riedel-de Haen (acetone), and Lab-scan (DMSO) origin were used. Solvents were dried before use by standard procedures [16].

The samples were taken in capillary tubes and their melting points were found by an electrochemical melting point apparatus Stuart SMP3. Elemental analyses were performed on a CHN-932 elemental analyzer, Leco Corporation, USA. Infrared spectra were recorded by a Perkin-Elmer-100 FTIR spectrophotometer from 4000 to 250 cm^{-1}. UV-absorption spectra were recorded by a double-beam UV–visible spectrophotometer, model 1601 made by the Shimadzu Company. As a light source, a deuterium lamp, 50-W halogen lamp, was used. Quartz cells having a path length of 1 cm were employed. The ^1H and ^{13}C NMR spectral measurements were made at 300 and 75 MHz, respectively, by a Bruker ARC 300 MHz-FT-NMR spectrometer. The EI mass spectra were recorded using a Thermo Fisher Exactive Orbitrap instrument, while electrospray ionization (ESI) mass spectrometry was performed by mass spectrometer LTQ XLTM linear ion trap (Thermo Scientific). TGA spectra were obtained by TGA-7 Perkin-Elmer USA under nitrogen.

The complexes were tested for their interactions with salmon sperm DNA (SS-DNA) [17, 18] and ALPs enzyme [19]. They were also screened to see their *in vitro* response against various strains of bacteria (*Escherichia coli*, *Bacillus subtilis*, *Staphlocuccus aureus,* and *Pasturella multocida*) and fungi (*Alternaria alternata*, *Ganoderma lucidum*, *Penicillium notatum,* and *Trichoderma harzianum*) by the disk diffusion method [20] and their minimum inhibitory concentrations (MIC) [21] were found. The antifungal/antibacterial activities were performed in an incubator (Sanyo, Germany) and sterilized in an autoclave (Omron, Japan). The MIC was determined in a Microquant apparatus (BioTek, USA). Streptomycin and fluconazole were used as standard drugs for antibacterial and antifungal screening tests, respectively. The *in vitro* hemolytic bioassays [22] of the complexes were performed with human red blood cells and the average lysis was reported with respect to the triton X-100 as positive control (100% lysis) and PBS as negative control (0% lysis).

2.2. *Synthesis of 1*

HLH (2 mM) was stirred with a solution of KOH (4 mM) in methanol (30 mL) in a 250 mL round-bottom flask for 0.5 h. Then CS_2 (2 mM) was added dropwise and stirred for 1.5 h at room temperature. To this mixture, a solution of $PdCl_2$ (1 mM) in water (50 mL) was added dropwise. The reaction mixture was vigorously stirred for 1 h. The solvent was removed under reduced pressure using a rotary evaporator to yield **1** [equation (1)].

(Equation 1)
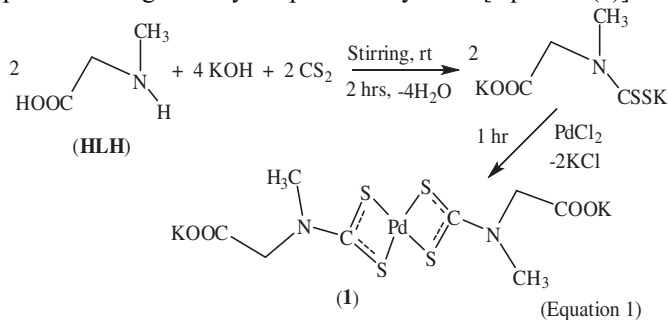
2.3. *Synthesis of 2–7*

A mixture of KOH (4 mM), HLH (2 mM) and CS_2 (2 mM) in methanol (10 mL) was stirred at room temperature for 2 h in a round-bottom flask (100 mL). Then R_2SnCl_2 or R_3SnCl (2 mM) was added as a solid with continuous stirring for 5 min. To this mixture, a $PdCl_2$ (1 mM) solution in methanol (100 mL) was added dropwise, and stirring was continued for further 2 h. The precipitates formed were filtered off and dried in air to yield **2–7** [equation (2)].

(Equation 2)
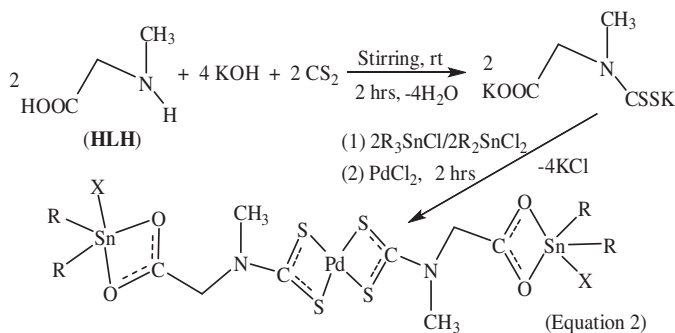
R = Me, X = Cl (**2**); R = Bu, X = Cl (**3**); R = Ph, X = Cl (**4**);

R = Me, X = Me (**5**); R = Bu, X = Bu (**6**); R = Ph, X = Ph (**7**)

3. Results and discussion

A palladium complex (**1**) was synthesized under basic conditions [23] by stirring sarcosine (HLH), KOH, and CS_2 in methanol at room temperature and then treating with an aqueous solution of $PdCl_2$. Heterobimetallic complexes **2–7** containing tin-carboxylate and

palladium-dithiocarbamate linkages were yielded by reacting potassium 2-(dithiocarboxyla-to(methyl)amino)acetate (prepared *in situ*) with R_2SnCl_2/R_3SnCl and then with $PdCl_2$. The products were produced in good yields and are stable in air. They are orange with sharp melting points. The palladated derivative **1** is soluble only in water but the heteronuclear (Sn, Pd) complexes are soluble in DMSO. Elemental (C, H, N, and S) analysis data agreed with the molecular formulas of the complexes.

3.1. *IR spectroscopy*

Infrared spectra of **1–7** were recorded from 4000 to 250 cm^{-1}. The most important bands are summarized in table 1. A peculiar feature of the IR spectrum of HLH is the appearance of a broad band at 3035 and 3710 cm^{-1} for vNH and vOH, respectively. Both these bands disappeared in KLCSSK and **1–7** indicating deprotonated –CSSH and –CSSH moieties. The vC–S and vN–CSS vibrational frequencies showed significant change after palladium–sulfur association. The vCS band at 975 cm^{-1} in KLCSSK was lowered to 960–968 cm^{-1} in **1–7** indicating metal–sulfur coordination which is also supported by appearance of vPd–S bands at 344–389 cm^{-1} [23]. The observed v(C–N) vibrations (1487–1585 cm^{-1}) in **1–7** lie between the values of 1250–1360 cm^{-1} and 1640–1690 cm^{-1} reported for C–N single bonds and C=N double bonds, respectively. Thus, v(N–CSS) (1487–1585 cm^{-1}) shifted to higher frequencies in complexes relative to the free ligand (KLCSSK) (1451 cm^{-1}) indicating the appearance of a partial double-bond character in dithiocarbamate and thus bidentate coordination with Pd(II) [24]. A symmetrical bidentate chelation of dithiocarbamate is verified by the appearance of a strong solitary C–S vibration at 960–968 cm^{-1} [25]. The absence of vPd–Cl vibrations in **1–7** describes the formation of dechlorinated-CSSPdSSC-type products; the formation of such products under specific (basic) reaction conditions is also supported by reported literature [23]. The free ligand (KLCSSK) exhibited vCOO$_{asym}$ and vCOO$_{asym}$ vibrations at 1660 and 1396 cm^{-1}, respectively. These two bands appeared at almost the same positions in **1** demonstrating non-coordinated COO–. The occurrence of $\Delta v = v$COO$_{(asym)} - v$COO$_{(sym)}$ values of 130–162 cm^{-1} suggested the bidentate binding mode of carboxylate in bimetallic **2–7** [26]. New bands at 422–467 cm^{-1} were observed for vSn–O vibrational modes indicating tin–carboxylate interaction in **2–7**. Bands at 550–572 cm^{-1} and 248–254 cm^{-1} were assigned to vSn–C vibrations in alkyltin(IV) and phenyltin(IV) moieties, respectively.

Table 1.   IR data^{a} (cm^{-1}) of HLH, KLCS$_2$ K and **1–7**.

Comp. No.	vNH$_{(str)}$	vOH	vCOO asym	vCOO sym	Δv	vC=N	vC=S	vSn–C	vSn–O	vSn–Cl	vPd–S
HLH	3035b	3710b	1621s	1407s	214	–	–	–	–	–	–
KLCS$_2$ K	–	–	1606s	1396s	210	1451m	975s	–	–	–	–
1	–	–	1598m	1385s	213	1487s	960s	–	–	–	389w
2	–	–	1594m	1464m	130	1508m	966s	565b	467w	280s	378m
3	–	–	1598m	1463w	135	1506s	963s	572m	422w	279s	346m
4	–	–	1586m	1430m	156	1585s	967s	254s	448w	290m	353w
5	–	–	1581s	1419w	162	1515s	965s	550s	441w	–	345s
6	–	–	1585s	1463w	122	1501s	968s	567m	463w	–	344s
7	–	–	1585s	1428s	157	1502s	966s	248s	445w	–	344s

^{a}Abbreviations: s, strong; m, medium; w, weak; b, broad.

3.2. *UV–visible spectroscopy*

UV–visible absorption spectra were recorded for the complexes at 1×10^{-5} M in DMSO from 200 to 800 nm at 25 °C. It was obvious from the spectra (figures 1 and 2) that such complexes with sulfur donor ligands are inactive in the visible region while each of the complexes exhibits a single sharp absorption in the UV region. A prominent strong band at 351 nm was assigned to a combination of intra-ligand and ligand-to-metal charge transfer absorptions and d–d bands, which support square planar palladium ions [27] in **1**. A square planar arrangement around Pd(II) is also supported in heterobimetallic complexes **2–7** due to occurrence of charge transfer transitions at 302–304 nm [28]. However, a decrease in absorption from 351 nm in **1** to 302–304 nm in **2–7** can be attributed to charge transfer from the ligand orbitals to the vacant orbitals of tin in **2–7** [29]. According to literature [30], three d–d spin-allowed singlet–singlet and three-spin-forbidden singlet–triplet transitions can be predicted for square planar complexes of palladium(II). However, strong
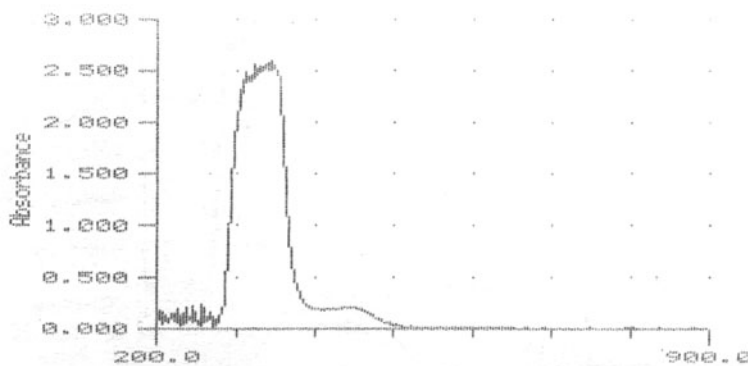

Figure 1.   UV–visible absorption spectrum of **1** recorded in 1×10^{-5} M DMSO solution at 25 °C.
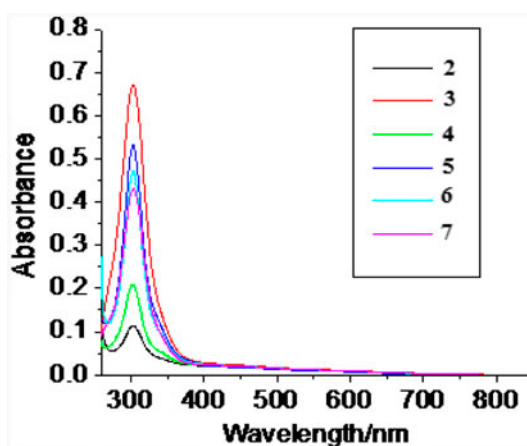

Figure 2.   UV–visible absorption spectra of **2–7** recorded in 1×10^{-5} M DMSO solution at 25 °C.

charge transfer transitions may interfere and prevent the observation of expected bands, especially for complexes containing sulfur donors. The availability of electrons on sulfur for electronic transition increases in the order **2 < 4 < 1 < 6 < 7 < 5 < 3**, increasing the molar extinction coefficient values [31].

3.3. ^1H NMR spectroscopy

^{1}H NMR spectra of the free ligand (HLH and KLCSSK) and **1–7** were recorded in deuterated water and DMSO, respectively, at room temperature. The number of protons found by integration agreed very well with those calculated from the expected composition. The ^{1}H NMR spectroscopic data are reported in table 2.

No resonances appeared for –COOH protons in ^{1}H NMR spectrum of HLH due to exchange of carboxylic proton with deuterium from D_2O. However, the absence of chemical shifts for –COOH and –CSSH protons recorded in deuterated DMSO for **1–7** indicates deprotonated carboxylic and dithiocarboxylic moieties. The methyltin(IV) protons in bimetallic **2** and **5** are a singlet at 1.87 and 0.42 ppm, respectively. The C−Sn−C bond angles (table 3) were calculated from $^2J(^{119}Sn-^1H)$ value [32]; the data strongly supports a five-coordinate geometry around tin(IV) in the chlorodimethyltin(IV) and trimethyltin(IV) centers in a coordinating solvent. The tin-bound methyl groups are axial (C−Sn−C = 152.2°) in **2** and equatorial (C−Sn−C = 119.3°, 117.9°) in **5** in solution. Despite the complex pattern of di- and tri-*n*-butyl fragments in the spectra of **3** and **6**, a clear triplet due to terminal methyl appeared at 0.85–0.86 ppm with $^3J(^1H, ^1H) = 7.20$ Hz. Ortho protons absorbed downfield when compared to meta and para protons in the phenyltin(IV) derivatives **4** and **7** [33].

3.4. ^{13}C NMR spectroscopy

^{13}C NMR spectra of free KLCS$_2$K and **1–7** were recorded in deuterated water and DMSO, respectively. The spectra displayed the expected carbon signals of the ligand skeleton and organotin(IV) moieties. The resonance signal for dithiocarbamate carbon of KLCS$_2$K shifted upfield from 211.4 ppm to 208.6–209.6 ppm in the complexes verifying palladium sulfur coordination. The –CSSPd chemical shifts were observed downfield when compared to those reported [34] for complexes having dithiocarbamate–tin interaction. The tin–carboxylate association was verified from the upfield shift of the resonance for –COO group from 176.4 ppm in the parent ligand salt (KLCS$_2$K) to 168.7–169.7 ppm in the synthesized products. A comparison of –CSS and –COO shifts before and after coordination clarifies that ^{13}C NMR signals of metal-bound carboxylate groups are shifted more upfield (6.7–7.7 ppm) than those of the coordinated dithiocarboxylate moieties (1.8–2.8 ppm), relative to their uncoordinated ligand. In other words, after coordination, the dithiocarbamate carbon is less shielded as compared to the carboxylate carbon, demonstrating that metal bonded with sulfur is more shielded when compared to that bonded with oxygen of the ligand. Thus, oxygen and sulfur donors of the ligand are coordinated with different metal centers (Sn and Pd) resulting in heterobimetallic complexes. The results agree with information obtained from IR, UV–visible, and mass spectroscopic data regarding Pd–sulfur and Sn–oxygen interactions. Due to involvement of both oxygen and sulfur for coordination, the neighboring methylene and methyl groups of the ligand skeleton also undergo upfield shifts in ^{13}C NMR spectra. The chemical shifts for methylene and methyl carbon of KLCS$_2$K were at 60.7 and 44.4 ppm, respectively, shifted upfield to 52.0–53.8 ppm and 38.1–38.4 ppm, respectively, in the corresponding complexes **2** and **4–6**.

Table 2. ^{1}H NMR chemical shifts^a (ppm) of the free ligands and **1**–**7**.

Proton No.	HLH	KLCS$_2$ K	Compound No.						
			1	2	3	4	5	6	7
1	2.48d	3.95s	2.79s	3.39d(9,6)	3.24s	3.26s	3.19s	3.19s	3.11s
2	3.15s	4.13s	3.30s	4.32s	4.35s	4.47s	4.14s	4.18s	4.25s
α	–	–	–	0.87s[103]	1.23–1.33m	–	0.42s[72/70]	1.06t(8.10)	–
β	–	–	–	–	1.54–1.59m	7.94d(7.2)[121/107]	–	1.51–1.62m	7.73–7.97m
γ	–	–	–	–	1.41–1.46m	7.81d(6.0)	–	1.22–1.34m	7.56–7.58m
δ	–	–	–	–	0.85t(7.2)	7.26–7.36m	–	0.86t(7.2)	7.27–7.45m

^{a}2J[$^{117/119}$Sn, ^{1}H] and ^{3}J(^{1}H, ^{1}H) are listed in square brackets and parenthesis, respectively; Multiplicity is given as: s = singlet, d = doublet, t = triplet, m = multiplet; The ^{1}H NMR numbering scheme of the ligand skeleton and the organotin moieties is as follows:
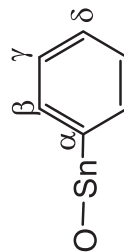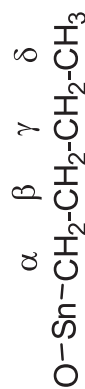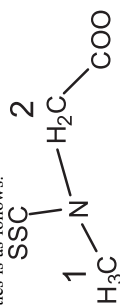
Table 3. (C–Sn–C) angles (°) based on ^{1}H and ^{13}C NMR parameters.

Comp. No.	$^2J(^{119/117}$Sn, ^{1}H) (Hz)	Angle (°) $\theta(^2J)$
2	103.5	152.2
5	72.0/69.9	119.3/117.9

3.5. *Mass spectrometry*

The electron ionization mass spectra (EI-MS) were recorded for **1** and **5**; **6** was investigated by ESI mass spectrometry. Complex **1** exhibited a very low intensity molecular ion peak [m/z = 510 (2%)] for [$C_8H_{10}K_2N_2O_4PdS_4$]$^+$ ion whose fragmentation started with the loss of one potassium to give [$C_8H_{10}KN_2O_4PdS_4$]$^+$ with m/z = 471 (1%). The decomposition pathways consisted of [$C_5H_5N_2PdS_4$]$^+$ [m/z = 327 (1%)] and [$C_2H_2NPdS_3$]$^+$ [m/z = 242 (1%)] fragments which recombined to yield [$C_7H_7N_3Pd_2S_7$]$^+$ with m/z = 569 (100%). Complex **5** undergoes EI-MS fragmentation to produce various tin and palladium-containing fragments verifying heterobimetallic (Sn, Pd) coordination. Primary fragmentation results in [SnMe$_3$]$^+$ [m/z = 165 (100%)] and [$C_6H_{11}N_2PdS_4$]$^+$ [m/z = 345 (43%)] species. Trimethyltin (IV) cation forms a base peak [m/z = 165 (100%)] and undergoes further fragmetation with loss of a methyl in each succeeding step to give ultimately the tin cation [m/z = 120 (10%)]. Complex **5** may also decompose into [$C_4H_7NO_2S_2Sn$]$^+$ [m/z = 285 (3%)] which loses a methyl radical and then an H$_2$S molecule to yield [$C_3H_2NO_2SSn$]$^+$ [m/z = 236 (1%)]. In ESI (positive mode) of **6**, the parent molecule either loses a methyl and a butyl substituent to yield [$C_{27}H_{52}N_2O_4PdS_4Sn_2$]$^+$ [m/z = 942 (52%)] or is protonated to produce an M + 1 peak of [$C_{32}H_{65}N_2O_4PdS_4Sn_2$]$^+$ [m/z = 1015 (61%)] which adopts three different routes for further disintegration. The base peak is for [$C_{21}H_{41}N_2PdS_4Sn_2$]$^+$ with m/z = 795 (100%). In negative mode, a peak at m/z = 1014 (64%) was assigned to the molecular ion (M) of **6**; the primary fragmentation occurred through the removal of a neutral molecule of either the butyl hydroxide or carbon dioxide to give corresponding peaks at m/z = 940 (41%) and 970 (34%), respectively. The secondary fragmentation proceeded through different pathways to produce anions completely matching the molecular skeleton of heterobimetallic (Sn, Pd) complex.

3.6. *Thermogravimetric analyses*

TGA of HLH and **2–4**, **6**, and **7** were performed under N$_2$ to evaluate degradation pattern, thermal stability, and percentage purity. The thermally decomposed data agreed well with the expected chemical composition of the ligand and complexes. Free HLH showed initial decomposition temperature of 182.2 °C and decomposed completely by 330 °C with continuous weight loss of almost 100%. The thermal stability of the complexes was higher than that of the free ligand since the increase in metal content makes a complex more resistant to decomposition [35]. The synthesized complexes were decomposed thermally by 600.8–820.0 °C to leave behind residual tin (SnO$_2$/SnO) and palladium (PdS/ Pd) deposits [36]. Thus, the TGA results are consistent with the heterobimetallic complexation of the products.

3.7. *DNA interaction studies*

DNA has generally been accepted as the target for most anticancer agents. Therefore, synthesizing a primary drug targeted toward DNA is considered an appropriate route to an anticancer drug discovery. UV–visible absorption spectroscopy is the simplest technique for studying both the stability of DNA and interaction with small molecules [37]. For the newly synthesized complexes, DNA-binding parameters were evaluated using absorption spectroscopy. The mode of interaction of the complexes with DNA was determined by comparison of absorbance and shifts in the wavelength range of 250–400 cm^{-1} with and without SS-DNA. The spectra were recorded at different DNA concentrations by keeping concentration of the complexes (2 mM) constant. Earlier reports [37] suggest that only the di- and triphenyltin(IV) complexes are active for binding with DNA, in most cases. However, all the newly synthesized Pd(II)/heterobimetallic products **1–7** interacted with DNA. The DNA binding of the complexes was attributed to the presence of Pd(II). However, in **4** and **7**, the phenyl moieties bound to tin may also play a significant role as phenyl facilitates interaction with double-stranded DNA [38]. There exists a single band in the absorption spectrum at 302.5 nm (**1**), 296.5 nm (**2**), 301 nm (**3**), 298.5 nm (**4**), 305.0 nm (**5**), 301.5 nm (**6**), and 300.0 nm (**7**). The UV spectra of complexes (figure 2) showed significant hypochromic effect and suggested mainly intercalating mode of binding. After 24 h, the spectrum was again taken with the same results which confirmed the stability of drug–DNA complex.

The intrinsic binding constants K for the investigated DNA active products were calculated to compare binding strengths of complex-DNA and ligand–DNA using the Benesi–Hildebrand equation (3) [39]:

$$\frac{A_0}{A - A_0} = \frac{\varepsilon_G}{\varepsilon_{H-G} - \varepsilon_0} + \frac{\varepsilon_G}{\varepsilon_{H-G} - \varepsilon_G} \times \frac{1}{K[DNA]} \tag{3}$$

where K, is the binding constant; A_0, is the absorbance of the drug; A, is the absorbance of the drug and its complex with DNA; ε_G, is the absorption coefficient of the drug; and ε_{H-G}, is the absorption coefficient of the drug–DNA complex. The association constants were obtained from the intercept-to-slope ratios of $A_0/(A - A_0)$ *versus* 1/[DNA] plots. The binding constants were 1.8×10^3 M^{-1} (**1**), 1.1×10^3 M^{-1} (**2**), 2.1×10^2 M^{-1} (**3**), 1.15×10^3 M^{-1} (**4**), 4.3×10^2 M^{-1} (**5**), 1.75×10^3 M^{-1} (**6**), and 1.51×10^3 M^{-1} (**7**). The UV studies (figure 3) demonstrated the highest value of binding constant for **1** due to its greater ability to bind with SS-DNA than the other complexes; tin coordination has decreased the binding power. The Gibb's free energy (ΔG) of the ligand and complexes were determined using equation (4):

$$\Delta G = -RT \ln K \tag{4}$$

The Gibb's free energies were −18.5 (**1**), −17.3 (**2**), −13.3 (**3**), −17.5 (**4**), −15.0 (**5**), −18.5 (**6**), and −18.1 (**7**) kJ M^{-1}. The negative values of ΔG suggest that the interaction of the compounds with DNA is spontaneous.

3.8. *ALPs activities*

The free ligand and the complexes were screened for their ALP activities. All the metal-coordinated products have activities. The inhibition of ALPs is caused due to palladium
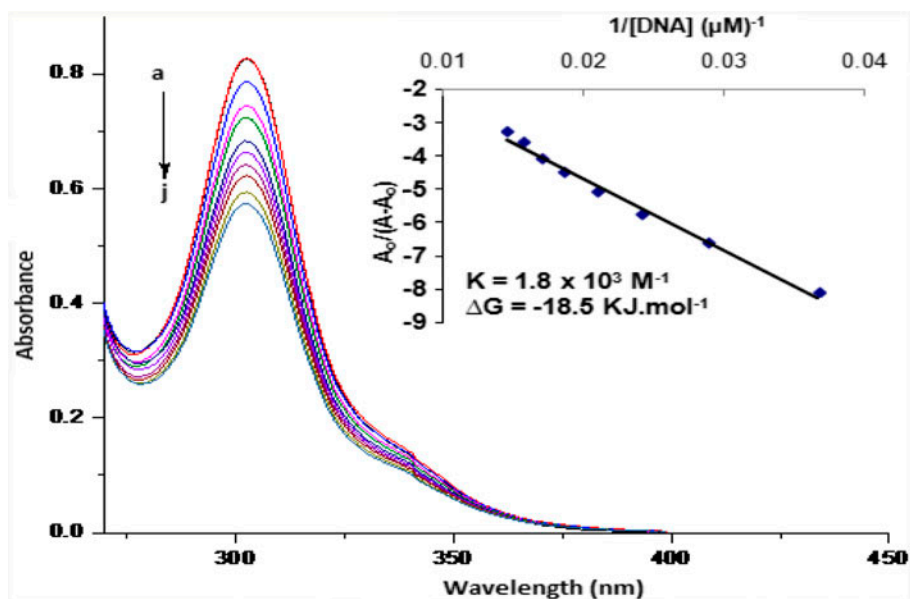
Figure 3.　Absorption spectra of 2 mM of **1** in the absence (a) and presence of 10 μM (b), 19 μM (c), 27 μM (d), 35 μM (e), 42 μM (f), 48 μM (g), 54 μM (h), 59 μM (i), and 64 μM (j) DNA. The direction of the arrow demonstrates increasing concentrations of DNA. Inside graph is the plot of $A_0/(A − A_0)$ vs. 1/[DNA] to find the Gibb's free energy and the binding constant of the DNA complex adduct.

coordination in the investigated complexes [40], causing blockage of active sites of the enzyme. The Pd may replace Zn or Mg of the enzyme and hence the enzyme fails to bind with the substrate. It is also possible that enzyme binds with the palladium complex or palladium ion more efficiently than substrate. The exact mechanism is still unknown.

　　The activity of the metal complexes against ALPs was attributed to palladium coordination as HLH was totally inactive and **1** was a potent ALPs inhibitor (figure 4). However,
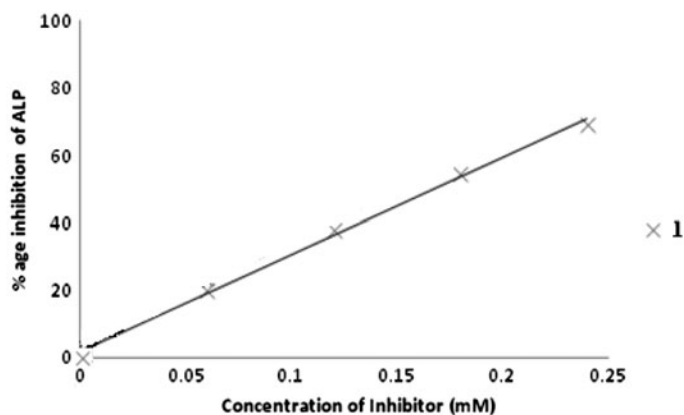

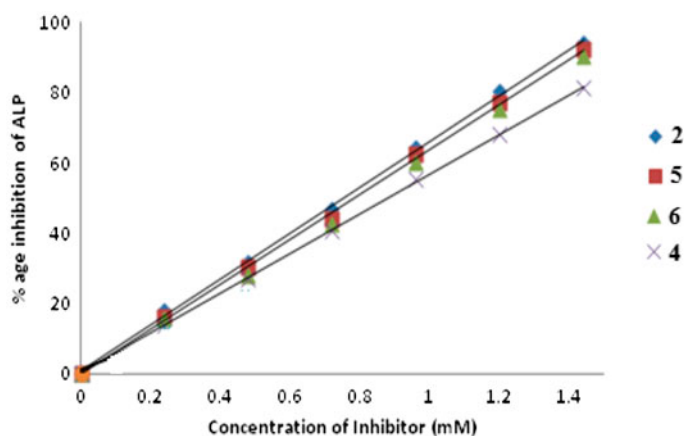Figure 4.　Concentration-dependent inhibition of ALPs by **1**.

Figure 5.   Concentration-dependent inhibition of ALPs by heteronuclear **2** and **4–6**.

the Sn(IV) association has decreased the activities, so **2** and **4–6** exhibited less activities against ALPs than **1**. Among the bimetallic products, the highest ALPs inhibition was observed for **2** (figure 5), arising from decreased steric interactions of two small tin-bound methyl groups. There was small decrease in activity with increasing size of the complex in going from **2** to **5** and **6** having three methyl and butyl groups, respectively, bound to tin. Complex **4** was less active due to phenyl groups bonded to tin, hindering the fitting of complex in the active sites of enzymes.

3.9. *Antimicrobial activities*

The ligands and complexes were screened for *in vitro* response against various strains of bacteria (*E. coli*, *B. subtilis*, *S. aureus,* and *P. multocida*) and fungi (*A. alternata*, *G. lucidum*, *P. notatum,* and *T. harzianum*). The antimicrobial activities were performed by disk diffusion method [20], followed by measurement of MIC [21]. Streptomycin and fluconazole were used as the positive controls for antibacterial and antifungal screening tests, respectively. Test sample/reference drug (1 mg/1 mL of solvent) [41] was introduced into the wells or disks. The wells exhibiting MICs were noted visually, while the zones of inhibition of disks were measured in millimeters. The data have been summarized in tables 4 and 5.

A close relationship was observed between structure and activity of the synthesized complexes. Each metal (Sn and Pd) plays a role in biological actions of such complexes. While palladium chiefly renders the capacity of DNA binding and ALPs inhibition in complexes, the coordination with tin enhances the antibacterial and antifungal potentials. Free HLH or KLCS$_2$K was totally inactive against the tested organisms. Coordination of ligand with Pd(II) in **1** has activities against some fungal microbes. However, heterobimetallic (Sn, Pd) complexation has antibacterial as well as antifungal activities with increase in biopotencies from **1**. In most cases, the complexes were more potent inhibitors of fungal culture when compared to bacterial growth, thus supporting earlier reports [42] relating to heterobimetallic (Sn, Pd) products. Moreover, the MIC values of such products were generally lower against fungi when compared to bacteria. The literature [43] shows that

Table 4. Antibacterial and antifungal activities data[a] (disk diffusion method).

Comp. No.	Bacterial inhibition zone (mm)				Fungal inhibition zone (mm)			
	E. coli	B. subtilis	S. aureus	P. multocida	A. alternata	G. lucidum	P. notatum	T. harzianum
HLH	—	—	—	—	—	—	—	—
KLCS$_2$ K	—	—	—	—	—	—	—	—
1	20 ± 0.18	16[bc] ± 0.06	20[bc] ± 0.16	—	13[c] ± 0.19	20[c] ± 0.08	—	20[bc] ± 0.14
2	—	18[bc] ± 0.14	20[bc] ± 0.32	—	16[bc] ± 0.08	23[bc] ± 0.17	—	14[c] ± 0.15
3	22[bc] ± 0.19	16[bc] ± 0.15	18[bc] ± 0.17	20[c] ± 0.24	18[bc] ± 0.12	28[bc] ± 0.19	28[bc] ± 0.17	25[b] ± 0.22
4	30[a] ± 0.20	20[bc] ± 0.19	30[ab] ± 0.21	22[bc] ± 0.11	14[bc] ± 0.19	20[c] ± 0.14	26[bc] ± 0.21	25[b] ± 0.13
5	21[bc] ± 0.13	20[bc] ± 0.18	18[bc] ± 0.19	—	17[bc] ± 0.11	—	18[c] ± 0.12	16[bc] ± 0.09
6	20[c] ± 0.18	14[c] ± 0.14	16[c] ± 0.20	20[c] ± 0.16	26[b] ± 0.21	30[b] ± 0.28	33[ab] ± 0.19	35[a] ± 0.27
7	—	—	—	20[c] ± 0.09	20[bc] ± 0.15	25[bc] ± 0.21	22[bc] ± 0.14	18[bc] ± 0.13
Standard drug	30[ab] ± 0.17	31[a] ± 0.28	31[a] ± 0.31	29[a] ± 0.28	38[a] ± 0.29	41[a] ± 0.21	45[a] ± 0.31	—

Notes: Values having same letters in superscripts of the same column do not differ significantly; 0 = no activity, 5–10 = activity present, 11–25 = moderate activity, 26–40 = strong activity; streptomycin, and fluconazole are standard antibacterial and antifungal drugs, respectively.

[a]Concentration = 1 mg mL^{-1} in DMSO; data are expressed as the mean ± standard deviation of samples analyzed individually in triplicate at $p < 0.1$.

Table 5.   Antibacterial and antifungal activities data[a] (minimal inhibitory concentration).

Comp. No.	MIC-bacterial ($\mu g\ mL^{-1}$)				MIC-fungal ($\mu g\ mL^{-1}$)			
	E. coli	B. subtilis	S. aureus	P. multocida	A. alternata	G. lucidum	P. notatum	T. harzianum
HLH	–	–	–	–	–	–	–	104
KLCS$_2$K	–	–	–	–	–	–	–	52
1	–	–	–	–	–	–	–	–
2	312	312	312	312	52	26	26	52
3	625	625	312	625	6.5	13	13	26
4	312	312	312	625	26	26	26	52
5	312	625	312	312	104	104	52	26
6	156	39	1.56	39	6.5	0.8	3.2	>0.4
7	312	156	312	39	52	26	26	52
Standard drug	1.2	2.4	78	39	26	26	>0.4	416

[a]Streptomycin and fluconazole are standard antibacterial and antifungal drugs, respectively.

organotin(IV) complexes are biologically active with a few exceptions. However, it is quite difficult to compare the results of the antimicrobial screening with those reported earlier because of the different methodology and strains assayed; yet, in view of the biological significance associated with tin, promising biological activity has been depicted by the complexes studied herein [44]. There is a direct relation between the activity and the coordination environment around metals [45]. The structural studies (IR, EIMS, TGA, ^{1}H NMR, and UV–visible) revealed that the investigated complexes maintain their solid-state five-coordinate environment around tin(IV) and four-coordinate geometries around palladium(Pd) in solution and do not lose their structural integrities even in solution. The biological activities are varied according to the substitution pattern at tin [46] with tri-butyltin(IV) derivative **6** most potent inhibitor of fungi, while trimethyltin(IV) derivative **5** generally exhibited higher antibacterial activity. The triorganotin(IV) derivatives generally exhibited higher inhibitory effect than their dianalogs, which may be due to greater lipophil-icity and permeability through the cell membrane [47]. The mechanism of action is not yet fully understood, but it is assumed that organic ligands support the transport of active organotin moiety to the site of action where it is released by hydrolysis. The anionic ligand also plays an important role in determining the degree of activity of organotin compounds [48]. MIC values of the complexes reveal a strong difference in antimicrobial activities due to the nature of the substituent present on the Sn metal [42].

3.10. *Hemolytic activities*

Hemolytic activity was studied because, even if a compound possesses potent antimicrobial activities, its use in medicine will be impossible in the presence of hemolytic effects. Thus, *in vitro* hemolytic bioassays of the ligand and the complexes were performed with human red blood cells and the average lysis was reported with respect to the triton X-100 as a posi-tive control (100% lysis) and PBS as a negative control (0% lysis).

The complexes possess hemolytic activities which were lower than triton X-100 and higher than PBS. The hemolytic activities did not show any significant changes in most complexes relative to the free ligand precursor (HLH, KLCS$_2$K). However, the results obtained for **2** and **5** are very interesting. Among all the investigated products, bimetallic

derivative **2** having chlorodimethyltin(IV) exhibited the lowest hemolytic effects (17.55%), while **5** having trimethyltin(IV) exhibited the highest hemolytic activity (78.64%). The compounds showing the highest activity may also be considered for antitumor activity [49].

4. Conclusion

The oxygen and sulfur sites of the bifunctional ligand are coordinated to the metal centers bidentate. There is a trigonal bipyramidal environment around Sn(IV) and a square planar geometry around Pd(II) in the solid and solution states of the complexes. There is a transfer of charge from the ligand orbitals to the vacant orbitals of tin. Complex **1** exhibited more interaction with SS-DNA and greater inhibition of ALPs than the bimetallic products. However, the heteronuclear (Sn, Pd) derivatives **2–7** possessed significantly higher anti-fungal/antibacterial potential when compared to **1**. The complexes were found most potent inhibitors of fungi when compared to bacteria. The heterobimetallic derivative **2** having chlorodimethyltin(IV) exhibited the lowest hemolytic effects (17.55%), while **5** having trimethyltin(IV) exhibited the highest hemolytic activity (78.64%).

Acknowledgements

Supplementary data

Physical data of complexes **1–7** (table S1); UV–visible absorption data of complexes **1–7** (table S2); ^{13}C NMR chemical shifts (ppm) of the ligand KLCS$_2$K and complexes **2** and **4–6** (table S3); Mass spectral data of complexes **1**, **5**, and **6** (table S4); Thermal decomposition data of complexes **2–4** and **6** and **7** (table S5); Hemolytic activity data of the ligand (HLH, KLCS$_2$K) and complexes **1–7** (table S6); Mass fragmentation pattern of complex **6** (positive mode) (figure S7); Absorption spectra of 2 mM of complexes **2–7** in the absence (a) and presence of 10 μM (b), 19 μM (c), 27 μM (d), 35 μM (e), 42 μM (f), 48 μM (g), 54 μM (h), 59 μM (i), 64 μM (j), and 69 μM (k) DNA; Inside each graph is the plot of $A_0/(A - A_0)$ *vs* 1/[DNA] to find the Gibb's free energy and the binding constant of complex–DNA adduct (figures S8–S13).

References

[1] V. Balzani, A. Juris, M. Venturi, S. Campagna, S. Serroni. *Chem. Rev.*, **96**, 759 (1996).
[2] T. Morita, T. Arai, H. Sasai, M. Shibasaki. *Tetrahedron: Asymmetry*, **9**, 1445 (1998).
[3] M. Shibasaki, H. Sasai, T. Arai. *Angew. Chem. Int. Ed. Engl.*, **36**, 1236 (1997).
[4] K.A. Magnus, H. Ton-That, J.E. Carpenter. *Chem. Rev.*, **94**, 727 (1994).
[5] P. Fierens, G.V.D. Dunghen, W. Segers, R.V. Elsuwe. *React. Kinet. Catal. Lett.*, **85**, 179 (1978).
[6] R. Gachter, H. Muller, *Plastics Additives Handbook*, 281, Hanser Publisher, Munich (1990).
[7] C. Gaina, V. Gaina, M. Cristea. *J. Inorg. Organomet. Polym.*, **19**, 157 (2009).
[8] S.K. Hadjikakou, N. Hadjiliadis. *Coord. Chem. Rev.*, **253**, 235 (2009).
[9] S.K. Hadjikakou, I.I. Ozturk, M.N. Xanthopoulou, P.C. Zachariadis, S. Zartilas, N. Hadjiliadis. *J. Inorg. Biochem.*, **102**, 1007 (2008).
[10] G.S. Drummond, A. Kappas. *Science*, **217**, 1250 (1982).
[11] A. Garoufis, S.K. Hadjikakou, N. Hadjiliadis. *Coord. Chem. Rev.*, **253**, 1384 (2009).
[12] D.Y. Ma, L.X. Zhang, X.Y. Rao, T.L. Wu, D.H. Li, X.Q. Xie. *J. Coord. Chem.*, **66**, 1486 (2013).
[13] M.I. Moghaddam, H.M. Torshizi, A. Divsalar, A.A. Saboury. *J. Iran. Chem. Soc.*, **6**, 552 (2009).

[14] H.M. Torshizi, M.I. Moghaddam, A. Divsalar, A.A. Saboury. *J. Biomol. Struct. Dyn.*, **26**, 575 (2009).
[15] A.C.F. Caires, E.T. Almeida, A.E. Mauro, J.P. Hemerly, S.R. Valentini. *Quim. Nova*, **22**, 329 (1999).
[16] W.L.F. Armarego, C.L.L. Chai. *Purification of Laboratory Chemicals*, 5th Edn, Butterworth Heinemann, London (2003).
[17] Y. Zhang, X. Wang, L. Ding. *Nucleos. Nucleot. Nucl.*, **30**, 49 (2011).
[18] C.V. Sastri, D. Eswaramoorthy, L. Giribabu, B.G. Maiya. *J. Inorg. Biochem.*, **94**, 138 (2003).
[19] M.R. Malik, V. Vasylyeva, K. Merz, N. Metzler-Nolte, M. Saleem, S. Ali, A.A. Isab, K.S. Munawar, S. Ahmad. *Inorg. Chim. Acta*, **376**, 207 (2011).
[20] The Clinical Laboratory Standards Institute (CLSI). *J. Clin. Microbiol.*, **45**, 2758 (2007).
[21] S.D. Sarker, L. Nahar, Y. Kumarasamy. *Methods*, **42**, 321 (2007).
[22] P. Sharma, J.D. Sharma. *J. Ethnopharmacol.*, **74**, 239 (2001).
[23] R.V. Singh, N. Fahmi, M.K. Biyala. *J. Iran. Chem. Soc.*, **2**, 40 (2005).
[24] D. Fregona, L. Giovagnini, L. Ronconi, C. Marzano, A. Trevisan, S. Sitran, B. Biondi, F. Bordin. *J. Inorg. Biochem.*, **93**, 181 (2003).
[25] F. Bonati, R. Ugo. *J. Organomet. Chem.*, **10**, 257 (1967).
[26] G.B. Deacon, R. Phillips. *J. Coord. Chem. Rev.*, **33**, 227 (1980).
[27] P.I.S. Maia, A. Graminha, F.R. Pavan, C.Q.F. Leite, A.A. Batista, D.F. Back, E.S. Lang, J. Ellena, S.S. Lemos, H.S. Salistre-De-Araujo, V.M. Deflon. *J. Braz. Chem. Soc.*, **21**, 1177 (2010).
[28] L.J. Al-Hayaly, N.H. Buttrus, F. Tarq, T.A.K. Al-Allaf. *Jordan. J. Appl. Sci.*, **17**, 64 (2005).
[29] N.H. Buttrus, K.S. Al-Numa, A.F. Mohammed. *Jordan. J. Appl. Sci.*, **10**, 71 (2008).
[30] A.I. Matesanz, J.M. Pérez, P. Navarro, J.M. Moreno, E. Colacio, P. Souza. *J. Inorg. Biochem.*, **76**, 29 (1999).
[31] T. Mukherjee, S. Sarkar, J. Marek, E. Zangrando, P. Chattopadhyay. *Transition Met. Chem.*, **37**, 155 (2012).
[32] T.P. Lockhart, W.F. Manders, E.M. Holt. *J. Am. Chem. Soc.*, **108**, 6611 (1986).
[33] S. Hussain, S. Ali, S. Shahzadi, S.K. Sharma, K. Qanungo, I.H. Bukhari. *J. Coord. Chem.*, **65**, 278 (2012).
[34] S. Hussain, S. Ali, S. Shahzadi, S.K. Sharma, K. Qanungo, M. Altaf, H.S. Evans. *Phosphorus, Sulfur Silicon Relat. Elem.*, **186**, 542 (2011).
[35] S.B. Kalia, G. Kaushal, K. Lumba, Priyanka. *J. Therm. Anal. Calorim.*, **91**, 609 (2008).
[36] Z.B. Leka, V.M. Leovac, S. Lukić, T.J. Sabo, S.R. Trifunović, K.M. Szécsényi. *J. Therm. Anal. Calorim.*, **83**, 687 (2006).
[37] F. Javed, S. Ali, M.W. Shah, K.S. Munawar, S. Shahzadi, Hameedullah, H. Fatima, M. Ahmed, S.K. Sharma, K. Qanungo. *J. Coord. Chem.*, **67**, 2795 (2014).
[38] M. Tariq, S. Ali, N. Muhammad, N.A. Shah, M. Sirajuddin, M.N. Tahir, N. Khalid, M.R. Khan. *J. Coord. Chem.*, **67**, 323 (2014).
[39] M.S. Ahmad, M. Hussain, M. Hanif, S. Ali, B. Mirza. *Molecules*, **12**, 2348 (2007).
[40] T.Z. Liu, L.Y. Chou, M.H. Humphreys. *Toxicol. Lett.*, **4**, 433 (1979).
[41] M.M. Amin, S. Ali, S. Shahzadi, S.K. Sharma, K. Qanungo. *J. Coord. Chem.*, **64**, 337 (2011).
[42] M. Rafiq, S. Ali, S. Shahzadi, M. Shahid, S.K. Sharma, K. Qanungo. *J. Iran. Chem. Soc.*, **11**, 169 (2014).
[43] S. Shahzadi, K. Shahid, S. Ali. *J. Coord. Chem.*, **60**, 2637 (2007).
[44] N. Sharma, V. Kumar, M. Kumari, A. Pathania, S.C. Chaudhry. *J. Coord. Chem.*, **63**, 3498 (2010).
[45] M.T. Anwar, S. Ali, S. Shahzadi, M. Shahid. *Russ. J. Gen. Chem.*, **83**, 2380 (2013).
[46] S. Hussain, S. Ali, S. Shahzadi, S.K. Sharma, K. Qanungo, M. Shahid. *Bioinorg. Chem. Appl.*, 11 (2014). Article ID 959203. doi:10.1155/2014/959203.
[47] Y. Shi, B.Y. Zhang, R.F. Zhang, S.L. Zhang, C.L. Ma. *J. Coord. Chem.*, **65**, 4125 (2012).
[48] K.C. Molloy, In *The chemistry of Metal–Carbon Bond*, F.E. Hartley (Ed.), Wiley, New York, NY (1989).
[49] A. Rehman, S.Z. Siddiqui, M.A. Abbasi, N. Abbas, K.M. Khan, M. Shahid, Y. Mahmood, M.N. Akhtar, N.H. Lajis. *Int. J. Pharm. Pharm. Sci.*, **676**, 4 (2012).